Delivering Mesenchymal Stem Cells in Collagen Microsphere Carriers to Rabbit Degenerative Disc: Reduced Risk of Osteophyte Formation

Yuk Yin Li, PhD,[1,*] Hua Jia Diao, PhD,[1,*] Tze Kit Chik, PhD,[1] Cin Ting Chow,[1] Xiao Meng An, PhD,[1] Victor Leung, PhD,[2] Kenneth Man Chi Cheung, MD,[2] and Barbara Pui Chan, PhD[1]

Mesenchymal stem cells (MSCs) have the potential to treat early intervertebral disc (IVD) degeneration. However, during intradiscal injection, the vast majority of cells leaked out even in the presence of hydrogel carrier. Recent evidence suggests that annulus puncture is associated with cell leakage and contributes to osteophyte formation, an undesirable side effect. This suggests the significance of developing appropriate carriers for intradiscal delivery of MSCs. We previously developed a collagen microencapsulation platform, which entraps MSCs in a solid microsphere consisting of collagen nanofiber meshwork. These solid yet porous microspheres support MSC attachment, survival, proliferation, migration, differentiation, and matrix remodeling. Here we hypothesize that intradiscal injection of MSCs in collagen microspheres will outperform that of MSCs in saline in terms of better functional outcomes and reduced side effects. Specifically, we induced disc degeneration in rabbits and then intradiscally injected autologous MSCs, either packaged within collagen microspheres or directly suspended in saline, into different disc levels. Functional outcomes including hydration index and disc height were monitored regularly until 6 months. Upon sacrifice, the involved discs were harvested for histological, biochemical, and biomechanical evaluations. MSCs in collagen microspheres showed advantage over MSCs in saline in better maintaining the dynamic mechanical behavior but similar performance in hydration and disc height maintenance and matrix composition. More importantly, upon examination of gross appearance, radiograph, and histology of IVD, delivering MSCs in collagen microspheres significantly reduced the risk of osteophyte formation as compared to that in saline. This work demonstrates the significance of using cell carriers during intradiscal injection of MSCs in treating disc degeneration.

Introduction

THE POTENTIAL OF USING mesenchymal stem cells (MSCs) to treat intervertebral disc (IVD) degeneration has been suggested in numerous animal models ranging from mice to cows.[1–24] In general, most if not all *in vivo* studies inject MSCs intradiscally in animals with induced disc degeneration. Enhanced matrix accumulation,[6,10,11,18,20] differentiation of MSCs into chondrogenic lineages,[6,8,10,18] and improvement in functional outcomes, such as disc height[7,11] and hydration index,[11] have been reported. Despite these encouraging results, the efficacy and safety of intradiscal injection of MSCs to treat disc degeneration have to be critically evaluated before well-designed clinical trials can be conducted. One long-lasting problem, which might cause suboptimal functional outcomes and adverse side effect of MSC-based therapy, is cell leakage.

During intradiscal injection, puncturing through the annulus into the cavity containing nucleus pulposus (NP) is necessary but the intradiscal pressure[25] in the disc would extrude the NP out. Therefore, the puncturing procedure itself has been used to induce disc degeneration[26] where magnetic resonance imaging (MRI) signal reduction, disc height reduction, and complications, such as herniation and osteophyte formation, are evident. Among the *in vivo* studies of MSC-based therapy in disc degeneration, most models inject cells in saline without a carrier[6,8–10,17,18,20] while others in hydrogel carriers, such as hyaluronic acid,[7,21] atelocollagen,[11] and fibrin.[19] However, backflow of the injected cells in saline is usually observed immediately after injection. Previous study reported that <1% of the labeled cells were detected in NP immediately after injection and a further significant reduction of injected cells was noted on day 7 even though a hydrogel carrier was used.[7] One primary

reason is the disc-pressure-induced extrusion of injected MSCs and the semifluid-like hyaluronic acid hydrogel, which has a viscosity of around 100 Pa, outside the disc space.[7] Recently, undesirable side effect of intradiscal injection of MSCs, namely, osteophyte formation, has been reported.[27] Specifically, injecting allogenic MSCs to degenerative disc in rabbit resulted in formation of large bony structures called osteophytes in all animals at 3 months postinjection,[27] corroborating with a previous report on osteophyte formation after MSC injection in healthy disc.[14] Most importantly, the link between cell leakage during intradiscal injection of MSCs and the side effect, osteophyte formation, has been suggested recently.[27] Labeled MSCs were not found in NP but within the osteophytes with endochondral ossification signs, providing evidences that the high intradiscal pressure may result in significant cell leakage during injection and the misdirected MSCs may contribute to the formation of osteophyte via chondrogenic differentiation.[27] These data raise the concerns on undesirable side effect or complication of MSC-based therapy in disc degeneration and suggest the significance of developing appropriate carrier system. Nevertheless, there is no comparative study to evaluate the potential benefit of delivering MSCs in a microcarrier, compared to delivering MSCs in saline alone.

We have developed a collagen microencapsulation platform, which entraps living cells in a solid microsphere made of biocompatible and biodegradable collagen nanofiber meshwork.[28] These solid microspheres have controllable size down to 100–300 μm in diameter and are injectable through syringe needles. These microspheres exhibit viscoelastic properties with a reduced elastic modulus of around 9 kPa,[29] matching well with the elastic modulus of NP, 10 kPa,[30] but differing from that of hydrogel, such as uncrosslinked hyaluronic acid (100 Pa),[7] collagen gel (132 Pa),[29] and crosslinked hyaluronic acid from commercial sources (<200 Pa for most and <1.2 kPa for a few highly crosslinked).[31] Moreover, these microspheres provide a 3D physiologically relevant scaffold for the encapsulated cells to attach to the collagen fibers via integrin-based adhesion[32] and can be localized at the injection site with retained cellular viability for at least 1 month.[28] Numerous cells, including MSCs,[28] embryonic stem cells,[33] chondrocytes,[34] HEK293 cells,[35] and NP cells,[36] have been microencapsulated in collagen microspheres. Cells encapsulated in collagen microspheres are able to survive, proliferate,[28,33,35] and migrate.[28] Encapsulated stem cells can undergo differentiation within the microspheres.[29,33,37–39] Further, mature cells, such as chondrocytes[34] and NP cells,[36] and differentiating stem cells, such as those toward chondrogenic[29,33,37] or osteogenic[38,39] lineage, are able to remodel the template matrix by depositing their own extracellular matrix and degrading the template collagen matrix,[29] demonstrating that the encapsulated cells can partially exhibit their physiological functions. Owing to these favorable properties, the collagen microsphere system has been used as 3D culture systems,[28,33,35,36,40] scaffolds for engineered tissues,[29,37–39] and miniaturized 3D microtissue models for studies of stem cell niche such as mechanical loading.[32,41] In this study, the role of collagen microspheres as an MSC carrier will be investigated using a rabbit disc degeneration model.

In this study, we hypothesize that intradiscal delivery of MSCs in solid collagen microspheres will show advantage over delivery of MSCs in saline, by improving functional outcomes and reducing side effect of osteophyte formation. Specifically, we aim to induce disc degeneration in rabbits, inject intradiscally autologous MSCs either in collagen microspheres or in saline, and evaluate the functional outcomes and side effect by radiographical, histological, biochemical, and biomechanical methods.

Materials and Methods

All protocols involving animals were approved by the committee for the use of Live Animals in Teaching and Research of the University of Hong Kong. Twenty-two 3-month-old New Zealand White rabbits were used for autologous MSC isolation, culture, encapsulation, and subsequent disc degeneration model with MSC reimplantation.

Isolation and culture of rabbit bone marrow MSCs

Under general anesthesia, 5 mL of bone marrow was aspirated from the disinfected medial proximal tibia of rabbits using an 18-gauge needle in a 10-mL syringe containing 2 mL of heparin (5000 IU/mL). The aspirate was fractionated by Ficoll density gradient centrifugation (GE Healthcare, Uppsala, Sweden) at 450 g for 30 min. The buffy coats were isolated and rinsed with phosphate-buffered solution (PBS) twice by centrifuging at 200 g for 10 min. The nucleated cells were cultured in growth medium consisting of Dulbecco's modified Eagle's medium high-glucose (DMEM-HG; Gibco, Grand Island, NY), 10% fetal bovine serum, 100 U/mL penicillin, 100 μg/mL streptomycin, 1.875 mg/mL sodium bicarbonate, 4.766 mg/mL 4-(2-hydroxyethyl)-1-piperazineethanesulfonic acid (HEPES), and 0.292 mg/mL L-glutamine. The medium was replenished 10 days after seeding and every 4 days thereafter. When approaching confluence, adherent cells were detached by 0.25% trypsin/1 mM EDTA and subcultured until P2 for subsequent experiments.

Microencapsulation of MSCs in collagen microspheres

MSC-collagen microspheres were prepared as described previously.[28] Briefly, an aliquot of 2.5×10^5 of MSCs at P2 were encapsulated in neutralized rat tail type I collagen solution (BD Biosciences, Bedford, MA) at a final concentration of 1 mg/mL in an ice bath. Droplets of 2 μL were pipetted onto a 100-mm-diameter Petri dish (Sterlin, Stone, United Kingdom) with UV-irradiated parafilm covering the substratum. After incubation of 30 min at 37°C, the gelated MSC-collagen microspheres were flushed with culture medium into the culture dish and cultured for 3 days before injection.

Disc degeneration model

Two months after bone marrow aspiration (5 months old), lumbar disc degeneration was induced by needle aspiration, modifying the procedures of previous report.[42] Under general anesthesia, the anterior surfaces of three consecutive lumbar IVDs (L2–L3 to L4–L5) were exposed through the retroperitoneal approach. Disc degeneration was induced by use of a 21-gauge needle to puncture the annulus fibrosus (AF) for a depth of 5 mm before aspirating out the NP tissue by pulling the plunger out completely at L2–L3 and L4–L5

levels. L3–L4 was left uninjured as the internal reference. Each rabbit was examined for the presence of NP within the syringe needle postinjection. The wound was closed in layers with absorbable sutures (Ethicon, Guaynabo, Puerto Rico). The rabbits were returned to their cages after complete awakening and freely mobilized.

Intradiscal injection of MSCs

One month after nucleus aspiration (6 months old), autologous MSCs previously prepared were transplanted back to the rabbits through an anterolateral approach as described previously.[42] Under general anesthesia and guided by radiograph, the retroperitoneal plane was dissected and the involved discs were exposed by separating the large psoas muscle. By pushing a 25-gauge needle coupled to a Hamilton syringe for 5 mm into the annulus, an aliquot of 2.5×10^5 of MSCs, either suspending in 20 µL of saline directly (MSCs in saline group), or encapsulated in collagen microspheres suspending in same volume of saline (MSC-collagen microsphere group), were randomly assigned and injected to degenerative disc levels L2–L3 or L4–L5, leaving the central L3–L4 intact as the uninjured internal reference group. The current study compares ''with'' and ''without'' the carriers, namely, collagen microsphere using uninjured level as an internal reference. No ''vehicle control'' was included in this study because the formation of MSC-collagen microsphere is a result of MSC-collagen matrix interaction during the process of microencapsulation and hence no ''MSC-free vehicle control'' can be prepared. Moreover, no ''injured but untreated'' group was included in this study because the potential benefits of MSC-based treatment in disc degeneration have been well demonstrated in numerous studies,[1–20] including our own.[6,12,42] Immediately after injection, the injection site was sealed with Histoacryl® glue (B. Braun, Melsungen, Germany) and the wounds were closed routinely. The rabbits were returned to their cages after complete awakening and allowed for free movement.

Radiographic analysis

MRI monitoring at preinjection (time 0), 1, 2, 3, and 6 months postinjection was conducted as previously reported.[43] Briefly, sagittal T2-weighted images of lumbar spine were taken using Siemens Magnetom Trio scanner (3T) in Hong Kong Sanatorium and Hospital. Mixtures of different ratios (10:0, 8:2, 6:4, 2:8, and 0:10) of deuterium oxide/water in cryotubes were scanned along with each rabbit as internal standard of hydration index (100%, 80%, 60%, 20%, and 0%) (Fig. 1A). A fish-oil capsule (Alaska; Nu-Health Products Co., Walnut, CA) was also scanned together to confirm that the fat suppression sequence was active. Syngo FastView tools were used to view the images (windowing at W:600 C:280) and serial images that contained signal from L2/L3, L3/L4, and L4/L5 levels were extracted analysis using the standard curve plotted using the deuterium oxide/water internal standards. Three to five slices were analyzed for each disc. Anterior–posterior X-ray radiographs of a rabbit spine were taken at predegeneration (−1), preinjection (0), 1, 2, 3, and 6 months postinjection using cabinet X-ray system (model 43855a; Faxitron, St, Lincolnshire, IL) with an exposure time of 18 s and penetration power of 45 kV. Disc height index (DHI) of rabbit
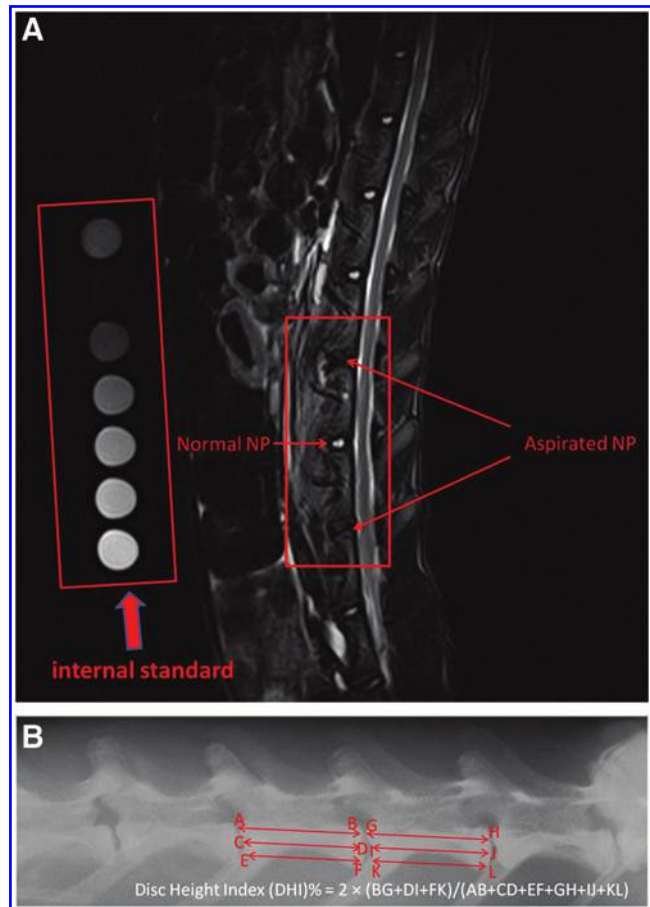

FIG. 1. Radiographic analysis of rabbit disc degeneration. **(A)** Representative magnetic resonance imaging (MRI) shows injured rabbit lumbar discs with internal standard for calibration of hydration index. **(B)** Representative X-ray radiograph showing the measurement of disc height index (DHI). Color images available online at www.liebertpub.com/tea

disc was calculated as previously described.[44] The change of DHI before and after MSC injection was expressed as %DHI (postinjection DHI/preinjection DHI) (Fig. 1B). All radiographs were examined for osteophyte formation as subsequently described.

Sample harvesting

Rabbits were sacrificed at 6 months postinjection. Three lumber levels of (L2/L3, L3/L4, and L4/L5) IVDs were harvested, wrapped in PBS-soaked gauze, and stored in a −80°C freezer until use. IVDs from 14 out of 22 rabbits were used for biomechanical evaluation followed by biochemical assessment while the rest 8 rabbits were used for histological analysis. After discarding the surrounding connective tissues, all specimens were examined again for the presence of osteophytes as subsequently described.

Biomechanical test

Two days before testing, disc specimens were thawed at 4°C overnight. The specimens were then potted in a 35-mm-diameter Petri dish using two-component epoxy paste adhesive (Araldite® AW2104/Hardener HW 2934, HUNTSMAN). A custom-made clamp was used to ensure that the specimens

were positioned in the center of the Petri dish and were parallel to the horizontal plane of the Petri dish. Specimens were then kept at 4°C overnight for setting of the epoxy adhesive with PBS. On the day of testing, potted specimens were tested in an ElectroForce® 5200 BioDynamic® test instrument (Bose Corporation, Eden Prairie, MN) by modifying a test protocol previously described.[45] In brief, PBS with protease inhibitors (1 mg/mL Pepstatin-A, 1 mM EDTA, 1 mM N-ethylmaleimide, and 1 mM benzamidine) was supplemented to the specimen containing Petri dish. The mechanical test was divided into five stages: (1) equilibration, (2) cyclic compression, (3) quasi-static compression, (4) frequency sweep, and (5) creep. Stage 1 consisted of a 30-min dwell at −10 N, targeting IVD stress of 0.1 MPa compression based on average rabbit IVD geometry (diameter: 10 mm, height: 5 mm). It acted as the minimum stress applied on specimens in subsequent tests. Stage 2 consisted of 20 cycles of sinusoidal compression at 1 Hz with an amplitude of 16.67 N centered about −26.67 N, which approximates the body weight of mature rabbit. Stage 3 included a slow compressive ramp at 0.005 N/s from −10 to −43.33 N applied on specimens. Stage 4 represented a dynamic mechanical analysis consisting of five cycles at five different frequencies: 0.05, 0.1, 0.5, 1, and 5 Hz applied from −10 to −43.33 N in sinusoidal compression. Finally in stage 5, the specimens were subjected to −66.67 N, which approximates 1.5 times of the body weight of mature rabbit, dwell for 30 min. A custom-made MATLAB code was used to analyze data collected in each stage to obtain relevant mechanical parameters. Displacement and time values collected in stages 1 and 5 were fitted to a stretched exponential function,[46]

$$d = (d_\infty - d_0)[1 - e^{-(t/\tau)^\beta}]$$

Where $(d_\infty - d_0)$ is the equilibrium height loss, t is time, τ is a time constant, and β is a stretch constant. Force and displacement values from the average of the 18th and 19th cycles measured in stage 2 were used to calculate the compressive stiffness using a linear regression. In stage 3, quasistatic stiffness was determined by linear regression of force–displacement data. The dynamic stiffness (K*) and the phase angle (δ) were obtained by fitting data into these functions,[47]

$$K^* = \left(\frac{F_0}{d_0}\right)e^{i\delta} \text{ and } \delta = \sin^{-1}\left(\frac{1}{2\pi}\int_{t_0}^{t_0+T} F\frac{dd}{dt}dt\right)$$

Where F is force, d is displacement, T is period, and t is time. Storage stiffness was calculated as $K^*\sin\delta$ while loss stiffness as $K^*\cos\delta$.

Biochemical evaluation

After the biomechanical test, the NP tissue of each IVD specimen was dissected out. Wet weight was measured followed by digestion in 600 mL of 300 µg/mL papain (Sigma-Aldrich, St. Louis, MO) in 50 mM phosphate buffer (pH 6.5), containing 5 mM L-cysteine and 5 mM EDTA at 60°C for 48 h.[48] Glycosaminoglycan (GAG) content of NP tissue was determined by the 1,9-dimethylmethylene blue (DMMB) method.[49] GAG concentration in specimens was calculated by calibrating against a standard curve using

shark chondroitin sulfate as standards (Sigma-Aldrich). Collagen content of NP tissue was determined by the hydroxyproline assay previously described.[29] The remaining papain digestion product was hydrolyzed in 2.6-fold volume of 6 N hydrochloric acid at 110°C for 16–18 h in a hydrolysis tube after being flushed with nitrogen gas for 30 s. The acid hydrolyzate was neutralized by 10 N sodium hydroxide. Trans-4-hydroxy-L-proline (Sigma-Aldrich) standards, ranging from 0 to 10 µg/mL hydroxyproline, were prepared. One hundred microliters of the standards and neutralized acid hydrolysate (pH 6–7) samples were added to a 96-well plate and incubated with 50 µL of 0.05 M chloramine T solution (Sigma-Aldrich) for 20 min at room temperature, followed by 50 µL of 3.15 M perchloric acid (Sigma-Aldrich) for 5 min at room temperature. Fifty microliters of 20% (w/v) p-dimethylaminobenzaldehyde solution (Sigma-Aldrich) was added and incubated for 20 min at 60°C for color development. The optical densities of standards and samples were measured at 557 nm using a microplate reader (UVM 340; ASYS Hitech GmbH, Eugendorf, Austria).

Histological and immunohistochemical evaluation

All three IVD levels of each rabbit were fixed in 4% PBS-buffered paraformaldehyde for 72 h, and then decalcified at 4°C in Morse's solution,[50] which is a mixture of equal volume of 45% formic acid and 20% sodium citrate, for 14 days. They were dehydrated step by step in gradient ethanol ranging from 50% to 100%, cleared in xylene, and embedded in paraffin wax. The embedded IVDs were cut into 8-µm-thick sections and stained with hematoxylin and eosin (H&E) and Alcian blue. Type II and type I collagens were also detected by immunohistochemistry using mouse primary antibodies against collagen II and collagen I (Calbiochem; dilution ratio 1:2000), respectively. After incubation at 4°C overnight, sections were incubated with goat anti-mouse secondary antibody (Dako, Hamburg, Germany) for 30 min, followed by incubation with avidin-biotin-peroxidase complex (Vector Laboratories, Burlingame, CA) for 30 min. Positive signal was visualized by diaminobenzidine (DAB; Dako). Hematoxylin was used for counterstaining. Histological examination on osteophyte formation was subsequently described.

Determination of osteophyte formation and calculation of odds ratio

Presence of osteophyte formation was collectively determined by X-ray radiographical analysis, physical examination, and histological confirmation. On radiographical evaluation, presence of signal outside the disc was regarded as osteophytes. On physical examination, presence of tissue outgrowth outside the disc was regarded as osteophyte. In some IVDs, both anterolateral and anterior osteophytes or "bridging osteophytes"[26] can be found in radiography that these osteophytes are usually larger than 2 mm in diameter and therefore are regarded as "large osteophytes." While in radiographs of other IVDs, only anterior osteophytes were detected that these osteophytes are usually smaller than 2 mm in diameter and therefore were regarded as "small osteopytes." On histological confirmation using saggital sections of the specimens, presence of tissue outgrowth outside AF was regarded as osteophyte formation. Positive

Alcian blue staining and collagen type II immunopositivity were used to define the cartilaginous nature of the outgrowth. The frequency of osteophyte formation in different groups was obtained to construct the contingency table. Odds ratio retrospectively measures the relative risk of having osteophytes when MSCs are delivered in a solid carrier (MSC-collagen microsphere) as compared with that without such a carrier (MSCs in saline). The odds ratio is defined as the ratio of odds of having osteophyte to having no osteophyte among specimens with the carrier, to the odds of having osteophyte to having no osteophyte among specimens without the carrier.

Statistical analyses

All quantitative data were expressed as mean ± standard error of mean or 95% confidence interval deviation unless otherwise specified. One-way or two-way ANOVA with repeated measurements or Bonferroni's *post hoc* tests were used to analyze radiographic measurements, extracellular matrix composition, and biomechanical properties. Linear

trend analysis was used to reveal the loading-frequency-dependent change in dynamic stiffness, storage stiffness, and loss stiffness of rabbit discs in phase 4 of the biomechanical test. Chi-square test was used to analyze the osteophyte frequency data on the association between osteophyte formation and treatment group while odds ratio was calculated to measure the relative risk of having osteophyte formation. IBM SPSS 19.0 was used to execute the analyses, and the significance level was set at 0.05.

Results

Temporal changes of hydration index and disc height

Figure 2A showed the MRI measurement on the hydration levels of different groups at different time points. Uninjured reference showed similar hydration index of around 40% throughout 6 months. The injured groups, injected with MSCs in saline or MSC-collagen microspheres, rapidly reduced the hydration level to 23% postinjury and the reduction leveled off, reaching about 10% at 6 months. General linear model with repeated measurements showed
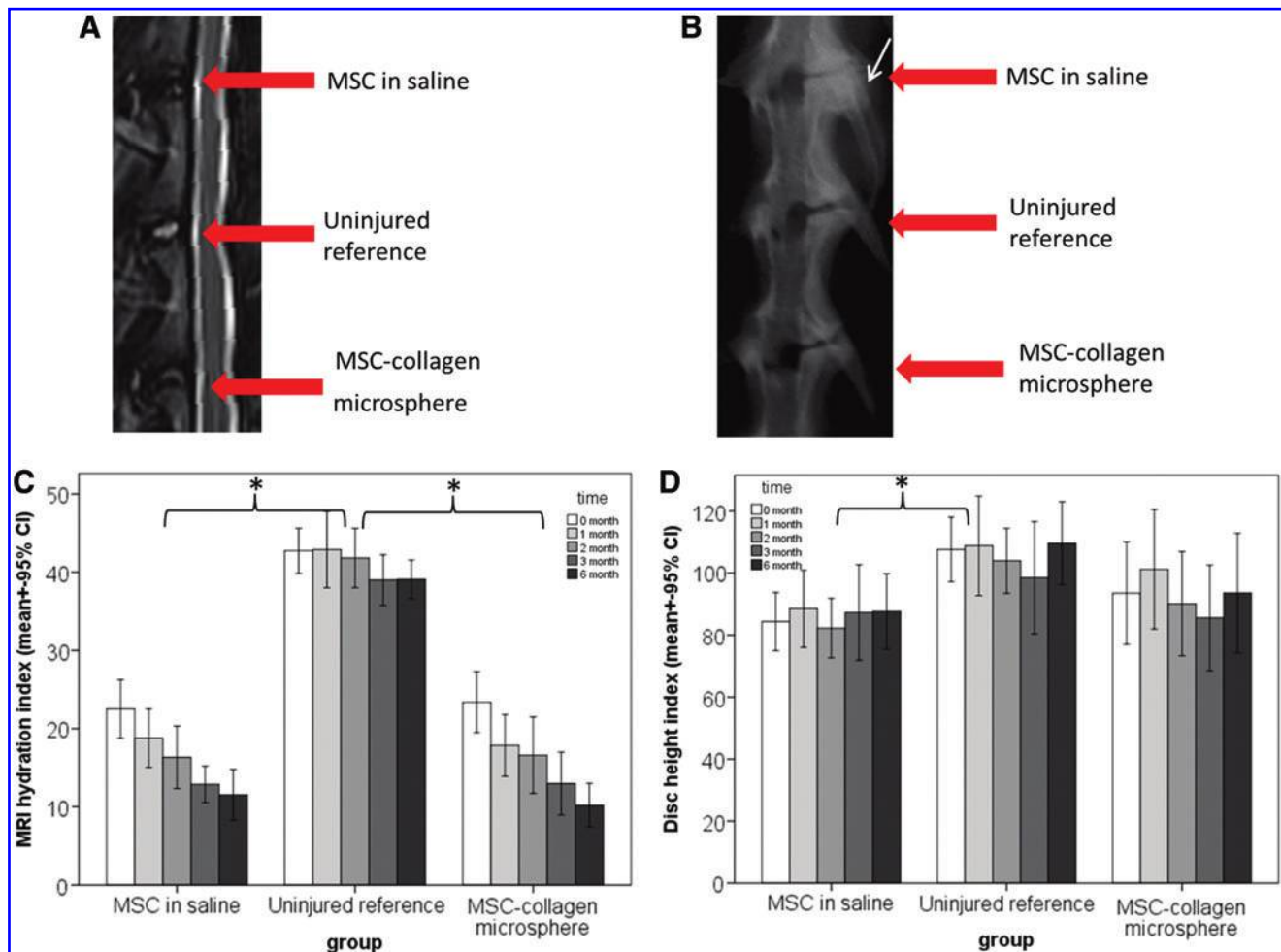

FIG. 2. MRI and X-ray radiographic analyses of rabbit disc after mesenchymal stem cell (MSC)–based treatment. **(A)** Representative T2-weighted MRI images showing the hydration signal; **(B)** representative X-ray images showing the disc height and osteophyte formation (white arrow); **(C)** bar chart showing the MRI hydration index of disc samples in various treatment groups at different time points; **(D)** bar chart showing the X-ray DHI of disc samples in various treatment groups at different time points ($n = 22$) (*$p < 0.05$). Color images available online at www.liebertpub.com/tea

that treatment group significantly affected the hydration index ($p<0.001$). Bonferroni's *post hoc* test showed that both the MSCs in saline group ($p<0.001$) and the MSC-collagen microsphere group ($p<0.001$) showed significant difference with the uninjured reference but not between themselves ($p=1.000$). Figure 2B showed DHI of different groups at different time points. The uninjured reference showed similar DHI of $\sim105\%$ throughout 6 months. The MSC-collagen microsphere group better maintained the disc height with a DHI of $>100\%$ at 1 month postinjury, accounting for $>95\%$ of the normal disc height, and of $>90\%$ throughout the rest of the monitoring period, accounting for $\sim86\%$ of the normal disc height. The MSCs in saline group maintained a DHI of $\sim85\%$ throughout 6 months, also accounting for $\sim80\%$ of the normal disc height. General linear model with repeated measurements showed that treatment group significantly affected the results ($p=0.043$) while Bonferroni's *post hoc* test showed that the difference between the MSCs in saline group and the uninjured reference was statistically significant ($p=0.042$). Nevertheless, the differences between the MSC-collagen microsphere group and the uninjured reference ($p=0.306$), and that between the two treatment groups ($p=1.000$) were insignificant.

Biomechanical performance of spinal motion segments

Table 1 summarized the mechanical parameters of the disc specimens in all groups and all stages of assessment at 6 months postinjury. In stages 1–3 and 5 of the mechanical analysis, no significant difference was detected among all three groups in biomechanical parameters, including phase angle at the same frequency, quasistatic stiffness, compressive stiffness, time constant, stretch constant, and creep height loss. In stage-4 dynamic compression analysis, Figure 3A showed the box plots of the dynamic stiffness of different groups under dynamic mechanical analysis at increasing frequencies from 0.05 to 5 Hz. The mean dynamic

stiffness in MSCs in saline group showed no increasing trend over ascending loading frequencies while that of both the MSC-collagen microsphere group and the uninjured control group increased as the frequency increases. One-way ANOVA with contrast showed that MSCs in saline group has no increasing trend over frequency ($p=0.214$) while both the MSC-collagen microsphere group ($p=0.031$) and the uninjured reference group ($p=0.012$) showed significant increasing trends as the loading frequency increased. Figure 3B showed the box plots of the storage stiffness of disc specimens versus loading frequency in log scale in different groups. Similarly, one-way ANOVA with contrast showed that the storage stiffness of MSCs in saline group showed no linear increasing trend with the log loading frequency ($p=0.285$) while the MSC-collagen microsphere group ($p=0.014$) simulated that of the uninjured reference group ($p=0.007$) by exhibiting a significant linear relationship with log loading frequency. Figure 3C showed the box plots of the loss stiffness in different groups. Significant linear relationship with log loading frequency was only demonstrated in the uninjured reference group ($p=0.002$) but not in the MSCs in saline group ($p=0.266$) and MSC-collagen microsphere group ($p=0.149$).

Biochemical matrix composition of NP

Figure 4 showed the extracellular matrix composition analysis in NP tissues retrieved from the disc specimens in different groups. The uninjured reference group showed the highest wet weight (Fig. 4A), GAG content (Fig. 4B), and the GAG:HYP ratio (Fig. 4D) but the lowest HYP collagen content (Fig. 4C) comparing with the MSCs in saline and MSC-collagen microsphere groups. The MSC-collagen microsphere group showed slightly higher wet weight and GAG content than the MSCs in saline group. One-way ANOVA with Bonferroni's *post hoc* tests showed that the differences between the MSCs in saline and the uninjured

TABLE 1. MECHANICAL ANALYSES OF SPINAL MOTION SEGMENTS OF DIFFERENT GROUPS

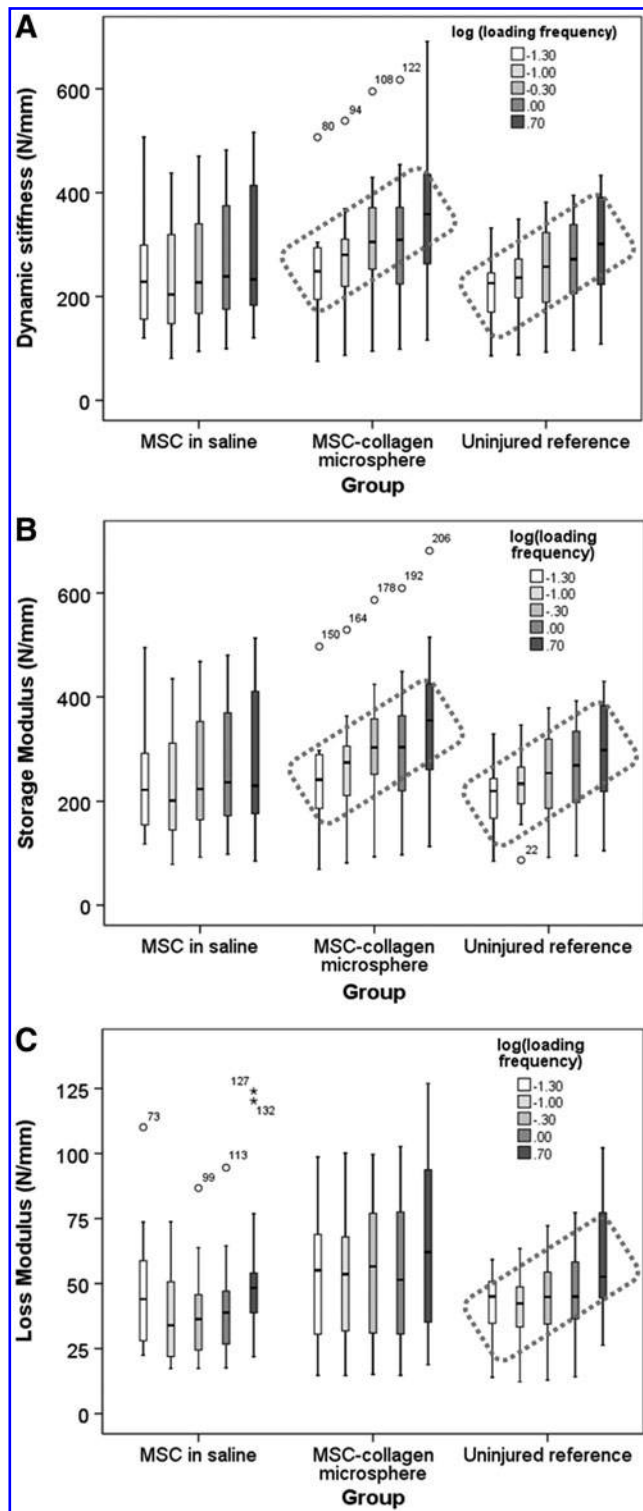| Test stage	Mechanical parameter	Control	rMSCs	rMSC-collagen microsphere
1. Equilibrium	$d_\infty - d_0$ (mm)	2.19 (0.42)	2.51 (0.33)	1.91 (0.34)
	Time constant	623 (212)	501 (164)	502 (187)
	Stretch constant	0.60 (0.08)	0.59 (0.07)	0.55 (0.07)
2. Cyclic compression	Compressive stiffness (N/mm)	260.18 (21.73)	238.60 (22.62)	272.69 (34.49)
3. Quasistatic compression	Quasistatic stiffness (N/mm)	91.10 (11.88)	85.07 (12.22)	82.60 (10.99)
	Height loss (mm)	0.49 (0.09)	0.51 (0.08)	0.51 (0.07)
4. Dynamic compression	Dynamic stiffness (N/mm)			
	0.05 Hz	217.16 (17.65)	250.75 (30.02)	242.51 (29.17)
	0.1 Hz	233.05 (18.68)	225.39 (27.76)	265.10 (31.59)
	0.5 Hz	254.61 (22.52)	244.12 (29.44)	303.96 (35.25)
	1 Hz	267.62 (23.43)	262.45 (31.70)	308.04 (36.74)
	5 Hz	301.22 (28.25)	286.29 (36.41)	357.87 (41.65)
	Phase angle (°)			
	0.05 Hz	11.25 (0.71)	11.16 (0.62)	12.78 (1.21)
	0.1 Hz	10.22 (0.69)	10.02 (0.61)	11.62 (1.10)
	0.5 Hz	10.15 (0.74)	9.46 (0.64)	10.98 (1.10)
	1 Hz	10.15 (0.76)	9.41 (0.67)	10.43 (1.00)
	5 Hz	12.56 (1.82)	13.48 (3.25)	10.81 (0.90)
5. Creep	$d_\infty - d_0$ (mm)	0.54 (0.08)	0.46 (0.06)	0.61 (0.13)
	Time constant	1499 (175)	1208 (234)	1010 (184)
	Stretch constant	0.48 (0.004)	0.48 (0.03)	0.50 (0.04)

FIG. 3. Summary of mechanical performance of rabbit degenerative discs. **(A)** Box plot showing the dynamic stress against loading frequency in rMSCs, control, and microsphere groups; **(B)** box plot showing the storage stiffness against loading frequency in log scale in MSCs in saline group, uninjured reference group, and MSC-collagen microsphere group; **(C)** box plot showing the loss stiffness against loading frequency in log scale in MSCs in saline group, uninjured reference group, and MSC-collagen microsphere group (red-dotted box: frequency-dependent trend).

reference as well as that between the MSC-collagen microsphere and the uninjured reference were statistically significant (all $p < 0.001$) but was insignificant between the two treatment groups ($p > 0.05$). For GAG content, the differences between the MSCs in saline group and the uninjured reference group as well as between the MSC-collagen microsphere group and the uninjured reference group were statistically significant (all $p \leq 0.002$) but were insignificant between the two treatment groups ($p > 0.05$). For HYP content, no statistical significance was found among all groups ($p > 0.05$). For GAG:HYP ratio, one-way ANOVA with Bonferroni's *post hoc* tests revealed significant differences between the MSCs in saline group and the uninjured reference group ($p = 0.001$) but not between the MSC-collagen microsphere group and the uninjured reference group ($p = 0.071$), as well as between the two treatment groups ($p > 0.05$).
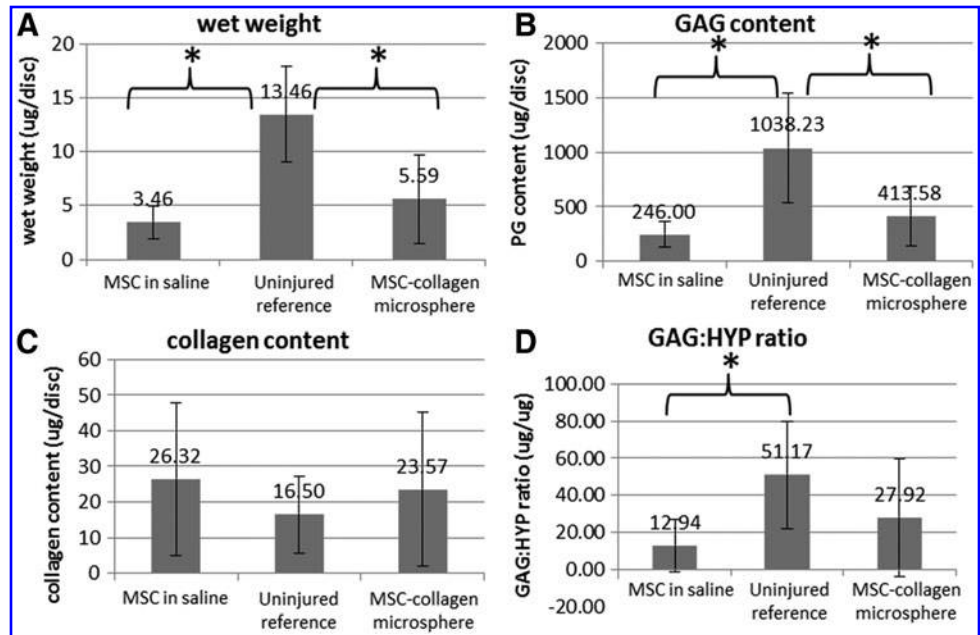
Histological and immunohistochemical evaluation of the disc

Figure 5 showed the morphological analysis and staining for NP matrices, including GAGs, type I collagen, and type II collagen. In general, the aspirated levels in both saline and microsphere groups showed shortened disc height while that of the uninjured reference showed no distortion of disc height. Upon H&E staining, AF of MSC-collagen microsphere group (Fig. 5C) showed regular arrangement, similar to that in the uninjured reference (Fig. 5B), while MSCs in saline group (Fig. 5A) showed that the inner AF invaded through the outer AF. Alcian blue staining for GAGs showed that the MSC-collagen microsphere group and the uninjured reference showed similar intensity (Fig. 5E, F) while that of the MSCs in saline group showed slightly lower intensity (Fig. 5D). Upon type I collagen immunohistochemistry, all groups showed similar staining (Fig. 5K–L) while small patches with type I collagen–immunopositive staining were found in the center of the NP region (Fig. 5L). These type I collagen patches were likely to be the type I collagen microspheres injected. Type II immunohistochemistry showed that AF of the normal control bulged outward because of the intact NP with high swelling pressure (Fig. 6N). On the other hand, the AF lamellae of the saline group were pressing inward, suggesting that the aspirated NP was not regenerated (Fig. 5M). In the MSC-collagen microsphere group (Fig. 5O), although the NP region was not as highly swollen as that of the uninjured reference (Fig. 5N), the AF lamellae were slightly bulging outward, indicating that the pressure was being built up. Moreover, there were patches of type II collagen–immunopositive regions at the center of NP, indicating that matrix remodeling at the type I collagen microspheres may occur.

Association between osteophyte formation and delivery method

Figure 6 tabulated the representative lateral X-ray radiographs and gross appearance of disc specimens in different groups. Specifically, Figure 6A showed the representative radiographs of disc specimens with and without osteophytes. For those with osteophytes, white arrows were used to indicate the presence of osteophytes. Disc specimens were

FIG. 4. Extracellular matrix composition of nucleus pulposus (NP) tissues of different groups. **(A)** Wet weight; **(B)** glycosaminoglycan (GAG) content; **(C)** HYP (marker of collagen) content; and **(D)** GAG:HYP ratio ($n = 14$) (*$p < 0.05$).

categorized as no identifiable osteophyte, small (< 2 mm), and large (> 2 mm) osteophytes. The number on the left lower corner of each category was the frequency of disc specimens in that category. Figure 6B showed the representative images of the gross appearance of disc specimens

with and without osteophytes. The disc specimens were cut into halves for retrieval of NP tissue for biochemical content analysis. Large tissue outgrowths were easily identified and were marked with asterisks while small osteophytes were identified as thin tissues that were not easily separated from
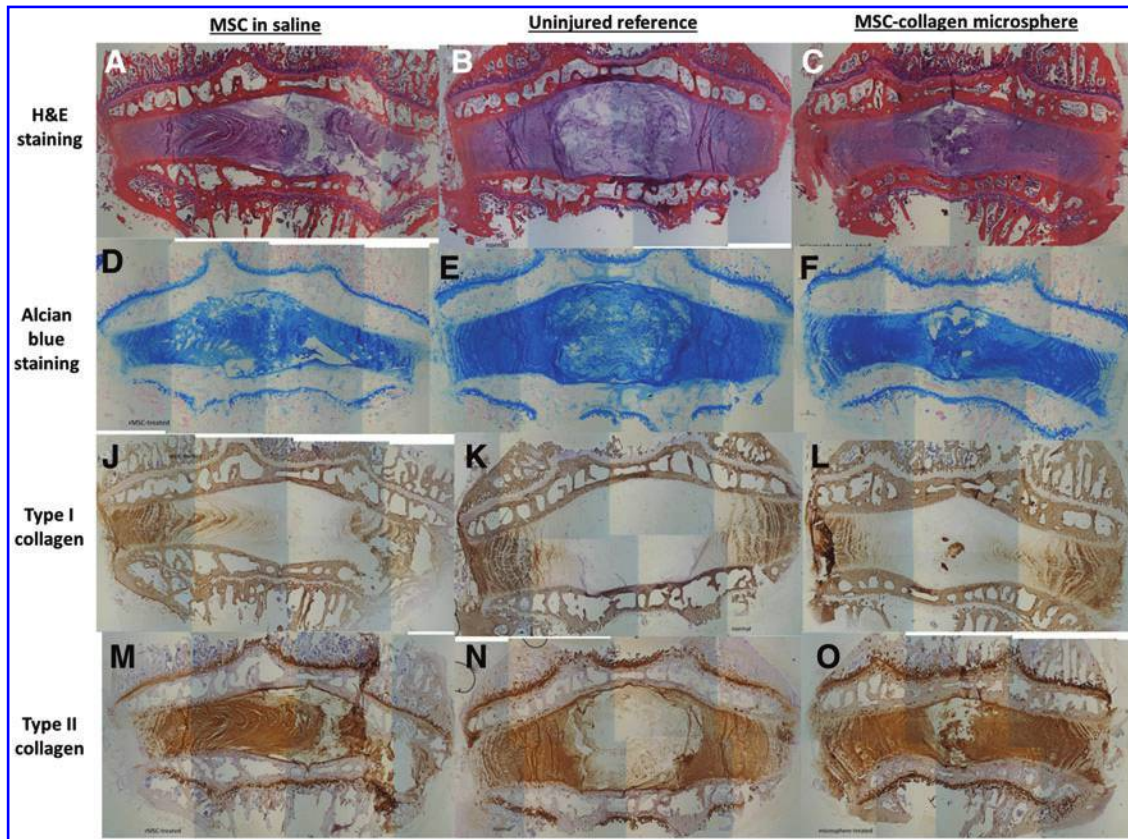

FIG. 5. Histology and immunohistochemistry of intervertebral disc (IVD) in different groups. **(A–C)** H&E staining; **(D–F)** Alcian blue staining; **(J–L)** type I collagen immunohistochemistry; **(M–O)** type II collagen immunohistochemistry; **(A, D, J, and M)** MSCs in saline group; **(B, E, K, and N)** uninjured reference group; **(C, F, L, and O)** MSC-collagen microsphere group. Color images available online at www.liebertpub.com/tea
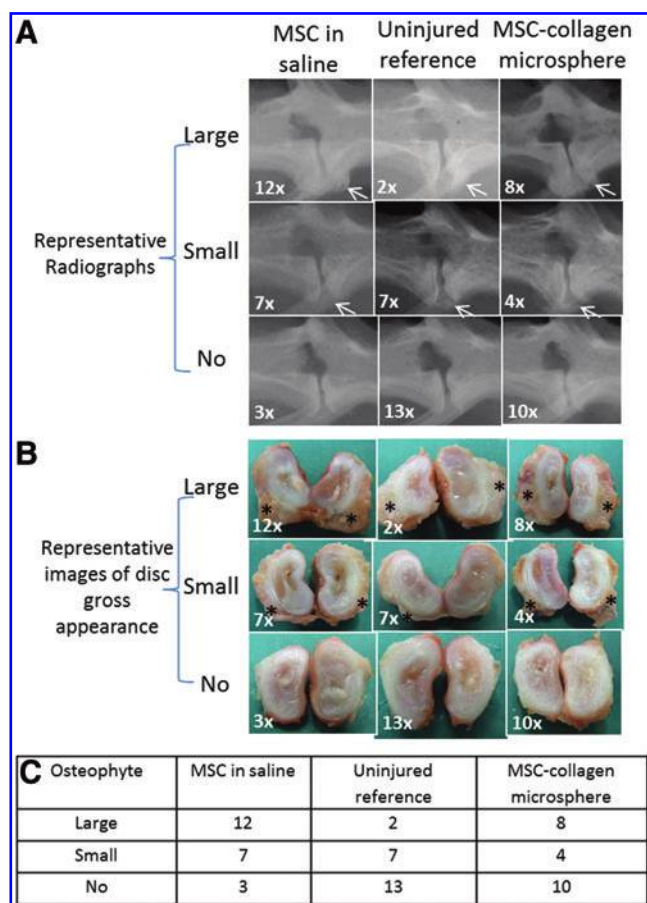
FIG. 6. Representative X-ray radiographs and gross appearance of IVD specimens with osteophytes of different sizes in different groups. **(A)** Radiographs; **(B)** gross appearance (the number on the lower left corner of each picture represents the frequency of specimens in that particular category); **(C)** contingency table of osteophyte formation versus different groups ($n = 22$). Color images available online at www.liebertpub.com/tea

the outer AF. Figure 6C showed the contingency table of the frequency of osteophyte formation (with different sizes) versus different groups (uninjured reference group, MSCs in saline group, and MSC-collagen microsphere group). In MSCs in saline group, 19 out of 22 IVDs (86.4%) showed osteophyte formation and most of them were large ones. In MSC-collagen microsphere group, 12 out of 22 IVDs (54.5%) showed osteophyte formation while the rest (10/22) were found no osteophyte. In uninjured reference group, 9 out of 22 IVDs (40.9%) showed osteophyte formation but most of them were small ones. Pearson Chi-square test showed that the treatment group variable significantly associated with the outcome measure (osteophyte formation; $p = 0.007$). Frequency data of osteophyte formation in the MSCs in saline group and the MSC-collagen microsphere group were used to calculate the odds ratio, which is the ratio of the odds of forming to not forming osteophyte among specimens with MSC-collagen microsphere, to the odds of forming to not forming osteophyte among specimens with MSCs in saline (i.e., without the carrier). This calculation requires an internal reference group and that was the uninjured reference group. The odds ratio calculated was 0.13, suggesting significantly

reduced odds of osteophyte formation among specimens with MSC-collagen microsphere, as compared with that without (i.e., MSCs in saline group).

Histological and immunohistochemical confirmation of osteophyte formation

Figure 7 showed the representative histological and immunohistochemical confirmation of osteophytes. In MSCs in saline group, large and rigid outgrowth structures (Fig. 7A) were easily identified while smaller osteophytes were identified in the MSC-collagen microsphere group (Fig. 7C). Osteophyte structure was not identified in the uninjured reference group (Fig. 7B). MSCs in saline group did not maintain an organized annulus lamellae structure at the anterior end where the injection was made and a large fibrous structure (green-dotted line) that continuously outgrows from the annulus could be identified (Fig. 7D). Numerous large-cell aggregates (asterisk) could be identified within the outgrowth, suggesting cell leakage (Fig. 7D). In MSC-collagen microsphere group, the annulus lamellae organization was well retained and a small patch of fibrous structure (green-dotted line) that discontinuously outgrows from the disc was identified (Fig. 7F). In the uninjured reference group, the annulus was intact (Fig. 7E). The IVD and the endplate regions of both the MSCs in saline group (Fig. 7G) and the MSC-collagen microsphere group (Fig. 7I) were all GAG rich as shown from the positive Alcian blue staining although the uninjured reference group showed most intensive staining (Fig. 7H). IVD in all groups showed weak immunopositivity for type I collagen (Fig. 7J–L), while both the IVD and the endplate of all groups showed intensive immunopositivity for type II collagen (Fig. 7M–O). The large outgrowth in the MSCs in saline group was largely immunopositive for type I collagen (green-dotted line, Fig. 7J) and partially immunopositive for both GAGs (green-dotted line, Fig. 7G) and type II collagen (green-dotted line, Fig. 7M), suggesting the fibrous and cartilaginous nature of the outgrowth and confirming the identity of the osteophyte. The small outgrowth in the MSC-collagen microsphere group was fibrous in nature as shown by the weak immunopositivity for type I collagen (green-dotted line, Fig. 7L) and negative staining for both GAG (Fig. 7I) and type II collagen (Fig. 7O).

Discussion

MSC-collagen microsphere group showed better dynamic mechanical behavior

Frequency-dependent changes in mechanical properties of spinal motion segment are important parameters in evaluating disc degeneration and emerging therapies.[51] Compression stiffness in healthy human spinal motion segment linearly increases as frequency increases in log scale.[51,52] Such frequency dependence of disc stiffness has been demonstrated in human discs[53,54] and pig discs.[55] This may be related to the stiffening effect and the fluid flow effect, which refers to more transport of fluid and ions and higher GAGs in central NP at high frequency as the disc is compressed.[51,56] This frequency-dependent change in dynamic stiffness was lost when the NP was removed by puncture injury[57,58] but the loss was prevented when injecting silicon polymers with suitable mechanical properties
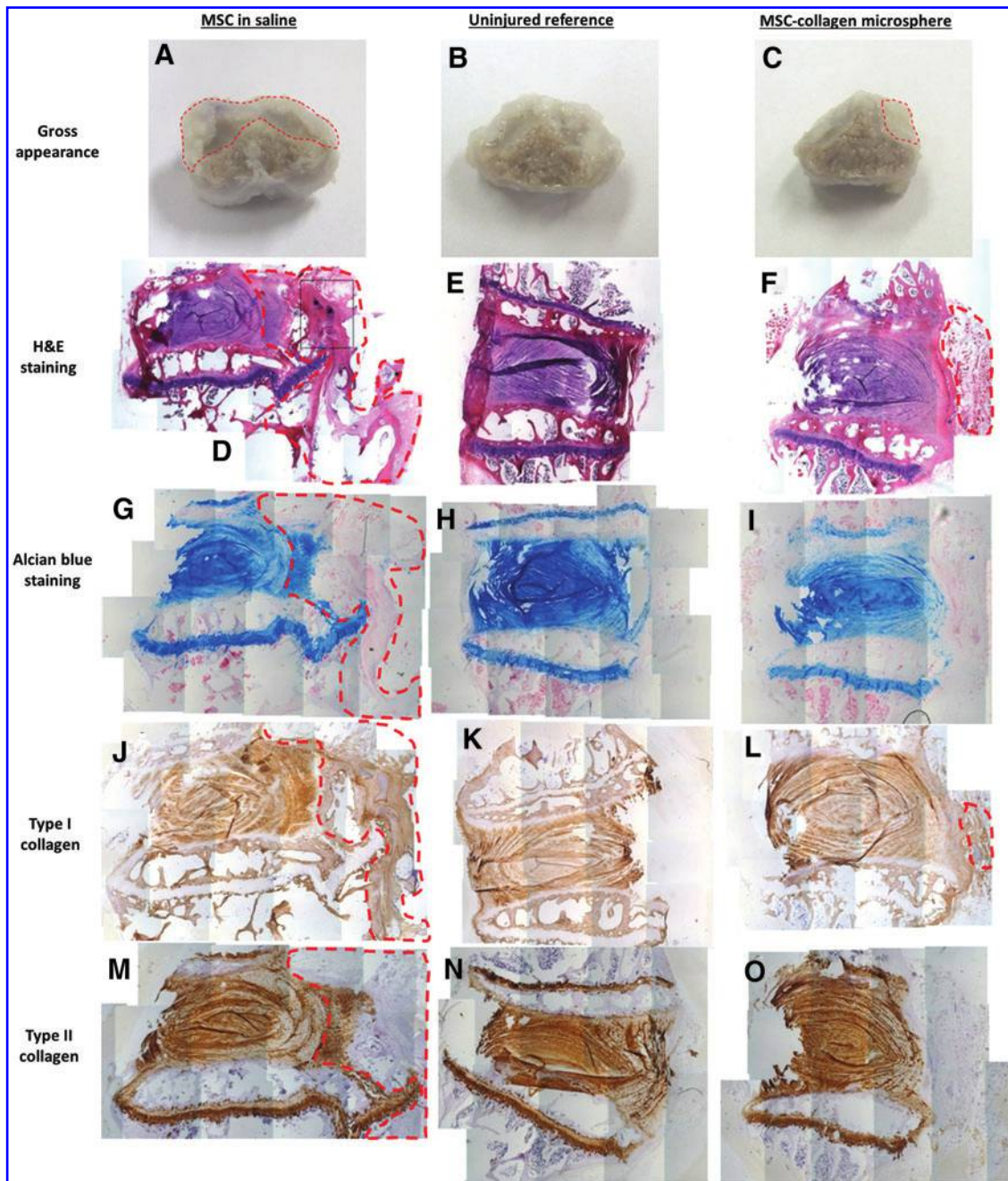
FIG. 7. Histological and immunohistochemical confirmation of osteophyte formation. **(A–C)** Gross appearance with indication of osteophyte formation (red-dotted line); **(D–F)** hematoxylin and eosin (H&E) staining with indication of the overgrowth structures (red-dotted line) and large-cell aggregates (asterisks); **(G–I)** Alcian blue staining for GAGs with indication of the cartilaginous outgrowth structure (red-dotted line); **(J–L)** immunohistochemical staining for type I collagen with indication of the fibrous outgrowth structures (red-dotted lines); **(M–O)** immunohistochemical staining of type II collagen with indication of the partially cartilaginous outgrowth (red-dotted line); **(A, D, G, J,** and **M)** MSCs in saline group; **(B, E, H, K,** and **N)** uninjured reference group; **(C, F, I, L,** and **O)** MSC-collagen microsphere group. Color images available online at www.liebertpub.com/tea

into the disc.[59] Moreover, frequency-dependent changes in disc dynamic stiffness have been associated with extracellular matrix component changes upon protease digestion and crosslinking treatment in rat spinal motion segments[45] while chondroitinase-ABC-induced degenerative disc was found with lower GAG content and lower dynamic stiffness,[60] both suggesting that dynamic mechanical analysis of the disc is a sensitive parameter revealing changes in matrix structural and compositional changes. In the current study, the presence of the collagen matrix and the fluid effect may produce a stiffening effect, contributing to the frequency-dependent dynamic mechanical properties. On the other hand, in the MSCs in saline group, the absence of collagen microsphere carrier results in a different structure and composition of NP, leading to distortion of the frequency dependence of the dynamic mechanical properties.

MSC-collagen microsphere group significantly reduced the risk of osteophyte formation

Osteophytes are bony projections formed along joint margins. It is a typical sign of disc degeneration.[26] Recently, osteophyte formation has been reported in all animals after intradiscal injection of MSCs to rabbit degenerative discs[27] and the presence of labeled MSCs within osteophytes with signs of endochondral ossification further suggests that cell leakage during intradiscal injection may be one of the causes for osteophyte formation. The current study reports the relative frequency of osteophyte formation in MSC-based treatments with and without carriers, using uninjured group as the internal reference. Osteophyte formation was found in ~40% of uninjured reference group although the majority is extremely small ones. This might be due to the change in mechanical environment after injuring two disc levels, above and beneath the uninjured level, therefore causing abnormal loading and degeneration over time. With collagen microspheres as the cell carrier, 50% of the injured discs showed osteophyte formation, while in MSCs in saline group, more than 86% showed osteophyte formation and the majority is large ones. The odds ratio measuring the relative risk of osteophyte formation in cases that deliver MSCs in collagen microspheres to cases that deliver MSCs in saline was 0.13. A less than unity odds ratio demonstrates reduced risks of osteophyte formation. One possible explanation is that the MSC-collagen microspheres are solid structures that are highly adhesive to tissues such that once they are delivered intradiscally, they can be easily localized to the disc, preventing cell leakage and the associated osteophyte formation. Nevertheless, further studies are needed to delineate the mechanism behind the reduced risk in osteophyte formation and to establish the causal relationship between cell leakage and osteophyte formation. Our results showed the significance of using cell carrier for intradiscal injection of MSCs in treating disc degeneration. Nevertheless, osteophyte formation was not completely eliminated in MSC-collagen microsphere group, suggesting that better methods to prevent osteophyte formation are warranted. Ongoing effort in developing an annulus plug that aims to completely block the injection portal and hence cell leakage is underway.

Limitations of the study

One limitation of this study is that the injected cells were not labeled and hence cell leakage could not be measured quantitatively. When injecting MSCs in saline intradically, backflow of liquids was observed immediately after the injection while when injecting MSC-collagen microspheres, no immediate backflow was observed. Since the study endpoint is 6 months postoperation, traditional fluorescence labels of cells would not work; future study on genetically labeling MSCs is warranted. Another limitation is the qualitative analysis of osteophyte formation. In this study, evaluation of osteophyte formation is based on qualitative examination of X-ray radiograph, physical inspection of the specimens, and histological confirmation. Therefore, only frequency data are available for analysis. To compare groups with different delivery methods using more powerful analyses, accurate measurement of osteophyte dimension is necessary. MicroCT imaging with volumetric analysis would be the ideal method to analyze the irregular-shaped osteophytes in a quantitative manner. Second, histological, biochemical, and mechanical evaluations of the discs before 6 months were not performed as we chose to monitor the degeneration and the efficacy of MSC injection using two clinically relevant, noninvasive, and nondestructive radiographic parameters, namely, X-ray disc height and MRI hydration index. As a result, any early differences in these parameters could not be revealed. Third, the current study used rabbit puncture injury model; similar to many other animal models for disc degeneration, it has limited representation of the natural etiology of disc degeneration in human. Moreover, many species, including rabbits, retain notochordal cells in the disc even after musculoskeletal maturation. Knowing these inevitable limitations using induced generation model in animals, further studies using more nature-mimicking models, such as the papain-induced degeneration model and species without notochordal cells such as bovine, are warranted.

Conclusions

This work demonstrates the significance of using cell carriers during intradiscal injection of MSCs in treating rabbit IVD degeneration. Comparing with delivering MSCs in saline, delivering MSCs in collagen microsphere carriers to degenerative disc showed better maintenance of dynamic mechanical performance and significant reduction in the risk of osteophyte formation, an unwanted complication associated with annulus damage and cell leakage during intradiscal injection.

Acknowledgments

Disclosure Statement

No competing financial interests exist.

References

1. Acosta, F.L., Jr., Lotz, J., and Ames, C.P. The potential role of mesenchymal stem cell therapy for intervertebral disc degeneration: a critical overview. Neurosurg Focus **19,** E4, 2005.
2. Leung, V.Y., Chan, D., and Cheung, K.M. Regeneration of intervertebral disc by mesenchymal stem cells: potentials, limitations, and future direction. Eur Spine J **15,** S406, 2006.
3. Wang, Y.T., Wu, X.T., and Wang, F. Regeneration potential and mechanism of bone marrow mesenchymal stem cell transplantation for treating intervertebral disc degeneration. J Orthop Sci **15,** 707, 2010.
4. Longo, U.G., Papapietro, N., Petrillo, S., Franceschetti, E., Maffulli, N., and Denaro, V. Mesenchymal stem cell for prevention and management of intervertebral disc degeneration. Stem Cells Int **2012,** 921053, 2012.
5. Drazin, D., Rosner, J., Avalos, P., and Acosta, F. Stem cell therapy for degenerative disc disease. Adv Orthop **2012,** 961052, 2012.
6. Yang, F., Leung, V.Y., Luk, K.D., Chan, D., and Cheung, K.M. Mesenchymal stem cells arrest intervertebral disc

degeneration through chondrocytic differentiation and stimulation of endogenous cells. Mol Ther **17,** 1959, 2009.

7. Crevensten, G., Walsh, A.J., Ananthakrishnan, D., Page, P., Wahba, G.M., Lotz, J.C., and Berven, S. Intervertebral disc cell therapy for regeneration: mesenchymal stem cell implantation in rat intervertebral discs. Ann Biomed Eng **32,** 430, 2004.

8. Wei, A., Tao, H., Chung, S.A., Brisby, H., Ma, D.D., and Diwan, A.D. The fate of transplanted xenogeneic bone marrow-derived stem cells in rat intervertebral discs. J Orthop Res **27,** 374, 2009.

9. Sakai, D., Mochida, J., Yamamoto, Y., Nomura, T., Okuma, M., Nishimura, K., Nakai, T., and Hotta, T. Transplantation of mesenchymal stem cells embedded in Atelocollagen gel to the intervertebral disc: a potential therapeutic model for disc degeneration. Biomaterials **24,** 3531, 2003.

10. Sakai, D., Mochida, J., Iwashina, T., Wantanabe, T., Nakai, T., Ando, K., and Hotta, T. Differentiation of mesenchymal stem cells transplanted to a rabbit degenerative disc model: potential and limitations for stem cell therapy in disc regeneration. Spine **30,** 2379, 2005.

11. Sakai, D., Mochida, J., Iwashina, T., Hiyama, A., Omi, H., Imai, M., Nakai, T., Ando, K., and Hotta, T. Regenerative effects of transplanting mesenchymal stem cells embedded in atelocollagen to the degenerated intervertebral disc. Biomaterials **27,** 335, 2006.

12. Cheung, K.M.C., Ho, G., Chan, D., and Leung, V.Y.L. Regeneration of nucleus pulposus after discectomy by autologous mesenchymal stem cells: a rabbit model. Eur Cells Mater **10,** 52, 2005.

13. Zhang, Y.G., Guo, X., Xu, P., Kang, L.L., and Li, J. Bone mesenchymal stem cells transplanted into rabbit intervertebral discs can increase proteoglycans. Clin Orthop Relat Res **430,** 219, 2005.

14. Sobajima, S., Vadala, G., Shimer, A., Kim, J.S., Gilbertson, L.G., and Kang, J.D. Feasibility of a stem cell therapy for intervertebral disc degeneration. Spine J **8,** 888, 2008.

15. Miyamoto, T., Muneta, T., Tabuchi, T., Matsumoto, K., Saito, H., Tsui, K., and Sekiya, I. Intradiscal transplantation of synovial mesenchymal stem cells prevents intervertebral disc degeneration through suppression of matrix metalloproteinase-related genes in nucleus pulposus cells in rabbits. Arthritis Res Ther **12,** R206, 2010.

16. Yang, H., Wu, J., Liu, J., Ebraheim, M., Castillo, S., Liu, X., Tang, T., and Ebraheim, N.A. Transplanted mesenchymal stem cells with pure fibrinous gelatin-transforming growth factor-beta1 decrease rabbit intervertebral disc degeneration. Spine J **10,** 802, 2010.

17. Feng, G., Zhao, X., Liu, H., Zhang, H., Chen, X., Shi, R., Liu, X., Zhao, X., Zhang, W., and Wang, B. Transplantation of mesenchymal stem cells and nucleus pulposus cells in a degenerative disc model in rabbits: a comparison of 2 cell types as potential candidates for disc regeneration. J Neurosurg Spine **14,** 322, 2011.

18. Henriksson, H.B., Svanvik, T., Jonsson, M., Hagman, M., Horn, M., Lindahl, A., and Brisby, H. Transplantation of human mesenchymal stems cells into intervertebral discs in a xenogeneic porcine model. Spine **34,** 141, 2009.

19. Acosta, F.L., Jr., Metz, L., Adkisson, H.D., Liu, J., Carruthers-Liebenberg, E., Milliman, C., Maloney, M., and Lotz, J.C. Porcine intervertebral disc repair using allogeneic juvenile articular chondrocytes or mesenchymal stem cells. Tissue Eng Part A **17,** 3045, 2011.

20. Hiyama, A., Mochida, J., Iwashina, T., Omi, H., Watanabe, T., Serigano, K., Tamura, F., and Sakai, D. Transplantation of mesenchymal stem cells in a canine disc degeneration model. J Orthop Res **26,** 589, 2008.

21. Ghosh, P., Moore, R., Vernon-Roberts, B., Goldschlager, T., Pascoe, D., Zannettino, A., Gronthos, S., and Itescu, S. Immunoselected STRO-3+ mesenchymal precursor cells and restoration of the extracellular matrix of degenerate intervertebral discs. J Neurosurg Spine **16,** 479, 2012.

22. Yoshikawa, T., Ueda, Y., Miyazaki, K., Koizumi, M., and Takakura, Y. Disc regeneration therapy using marrow mesenchymal cell transplantation: a report of two case studies. Spine **35,** E475, 2010.

23. Orozco, L., Soler, R., Morera, C., Alberca, M., Sánchez, A., and García-Sancho, J. Intervertebral disc repair by autologous mesenchymal bone marrow cells: a pilot study. Transplantation **92,** 822, 2011.

24. Kovacs, F.M., Abraira, V., Gérvas, J., Arana, E., Peul, W.C., Schoene, M.L., and Corbin, T.P. Overenthusiastic interpretations of a nonetheless promising study. Transplantation **93,** e6, 2012.

25. Roberts, S., Menage, J., Sivan, S., and Urban, J.P. Bovine explant model of degeneration of the intervertebral disc. BMC Musculoskelet Disord **9,** 24, 2008.

26. Sobajima, S., Kompel, J.F., Kim, J.S., Wallach, C.J., Robertson, D.D., Vogt, M.T. Kang, J.D., and Gilbertson, L.G. A slowly progressive and reproducible animal model of intervertebral disc degeneration characterized by MRI, X-ray, and histology. Spine **30,** 15, 2005.

27. Vadalà, G., Sowa, G., Hubert, M., Gilbertson, L.G., Denaro, V., and Kang, J.D. Mesenchymal stem cells injection in degenerated intervertebral disc: cell leakage may induce osteophyte formation. J Tissue Eng Regen Med **6,** 348, 2012.

28. Chan, B.P., Hui, T.Y., Yeung, C.W., Li, J., Mo, I., and Chan, C.G. Self-assembled collagen–human mesenchymal stem cell microspheres for regenerative medicine. Biomaterials **28,** 4652, 2007.

29. Li, C.H., Chik, T.K., Ngan, A.H., Chan, S.C., Shum, D.K., and Chan, B.P. Correlation between compositional and mechanical properties of human mesenchymal stem cell-collagen microspheres during chondrogenic differentiation. Tissue Eng Part A **17,** 777, 2011.

30. Iatridis, J.C., Weidenbaum, M., Setton, L.A., and Mow, V.C. Is the nucleus pulposus a solid or a fluid? Mechanical behaviors of the nucleus pulposus of the human intervertebral disc. Spine **21,** 1174, 1996.

31. Edsman, K., Nord, L.I., Ohrlund, A., Lärkner, H., and Kenne, A.H. Gel properties of hyaluronic acid dermal fillers. Dermatol Surg **38,** 1170, 2012.

32. Kwok, C.B., Ho, F.C., Li, C.W., Ngan, A.H.W., Chan, D., and Chan, B.P. Compression induced alignment and elongation of human mesenchymal stem cell (hMSC) in 3D collagen constructs is collagen concentration dependent. J Biomed Mater Res A **101,** 1716, 2013.

33. Yeung, C.W., Chan, D., Cheah, K., and Chan, B.P. Effects of reconstituted collagen matrix on fates of mouse embryonic stem cells before and after induction for chondrogenic differentiation. Tissue Eng Part A **15,** 3071, 2009.

34. Cheng, H.W., Tsui, K., Cheung, K.M.C., Chan, D., and Chan, B.P. Decellularization of chondrocyte-encapsulated collagen microspheres—A 3D model to study the effects of acellular matrix on stem cell fate. Tissue Eng Part C **15,** 697, 2009.

35. Wong, H.L., Wang, M.X., Cheung, P.T., Yao, K.M., and Chan, B.P. A 3D collagen microsphere culture system for GDNF-secreting HEK293 cells with enhanced protein productivity. Biomaterials **28,** 5369, 2007.

36. Yuan, M.T., Leong, K.W., and Chan, B.P. Three dimensional culture of rabbit nucleus pulposus cells in collagen microspheres. Spine J **11,** 947, 2011.

37. Hui, T.Y., Cheung, K.M., Cheung, W.L., Chan, D., and Chan, B.P. *In vitro* chondrogenic differentiation of human mesenchymal stem cells in collagen microspheres: influence of cell seeding density and collagen concentration. Biomaterials **29,** 3201, 2008.

38. Chan, B.P., Hui, T.Y., Wong, M.Y., Yip, H.K., and Chan, G.C.F. Mesenchymal stem cell-encapsulated collagen microspheres for bone tissue engineering. Tissue Eng Part C Methods **16,** 225, 2010.

39. Cheng, H.W., Luk, K., Cheung, K.M.C., and Chan, B.P. *In vitro* generation of osteochondral interface from mesenchymal stem cell-collagen microspheres. Biomaterials **32,** 1526, 2011.

40. Lee, M., Lo, A.C., Cheung, P.T., Wong, D., and Chan, B.P. Drug carrier systems based on collagen-alginate composite structures for improving the performance of GDNF-secreting HEK293 cells. Biomaterials **30,** 1214, 2009.

41. Au-yeung, K.L., Sze, K.Y., Sham, M.H., and Chan, B.P. Development of a micromanipulator-based loading device for mechanoregulation study of human mesenchymal stem cells in 3D collagen constructs. Tissue Eng Part C Methods **16,** 9, 2010.

42. Ho, G., Leung, V.Y., Cheung, K.M., and Chan, D. Effect of severity of intervertebral disc injury on mesenchymal stem cell-based regeneration. Connect Tissue Res **49,** 15, 2008.

43. Leung, V.Y., Hung, S.C., Li, L.C., Wu, E.X., Luk, K.D., Chan, D., and Cheung, K.M. Age-related degeneration of lumbar intervertebral discs in rabbits revealed by deuterium oxide-assisted MRI. Osteoarthritis Cartilage **16,** 1312, 2008.

44. Masuda, K., Aota, Y., Muehleman, C., Imai, Y., Okuma, M., Thonar, E.J., Andersson, G.B., and An, H.S. A novel rabbit model of mild, reproducible disc degeneration by an anulus needle puncture: correlation between the degree of disc injury and radiological and histological appearances of disc degeneration. Spine **30,** 5, 2005.

45. Barbir, A., Michalek, A.J., Abbott, R.D., and Iatridis, J.C. Effects of enzymatic digestion on compressive properties of rat intervertebral discs. J Biomech **43,** 1067, 2010.

46. Lakes, R.S. Constitutive relations. In: Kulacki FA, ed. Viscoelastic Solids. Boca Raton: CRC Press, 1998, pp. 15–62.

47. Findley, W.N., Lai, J.S., and Onaran, K. Linear Viscoelastic Constitutive Equations, Creep and Relaxation in Nonlinear Viscoelastic Materials. New York: Dover, 1989, pp. 90–96.

48. Miyamoto, K., Masuda, K., Kim, J.G., Inoue, N., Akeda, K., Andersson, G.B., and An, H.S. Intradiscal injections of osteogenic protein-1 restore the viscoelastic properties of degenerated intervertebral discs. Spine J **6,** 692, 2006.

49. Barbosa, I., Garcia, S., Barbier-Chassefiere, V., Caruelle, J.P., Martelly, I., and Papy-Garcia, D. Improved and simple micro assay for sulfated glycosaminoglycans quantification in biological extracts and its use in skin and muscle tissue studies. Glycobiology **13,** 647, 2003.

50. Leung, V.Y., Chan, W.C., Hung, S.C., Cheung, K.M., and Chan, D. Matrix remodeling during intervertebral disc growth and degeneration detected by multichromatic FAST staining. J Histochem Cytochem **57,** 249, 2009.

51. Costi, J.J., Stokes, I.A., Gardner-Morse, M.G., and Iatridis, J.C. Frequency-dependent behavior of the intervertebral disc in response to each of six degree of freedom dynamic loading: solid phase and fluid phase contributions. Spine (Phila Pa 1976) **33,** 1731, 2008.

52. Sen, S., Jacobs, N.T., Boxberger, J.I., and Elliott, D.M. Human annulus fibrosus dynamic tensile modulus increases with degeneration. Mech Mater **44,** 93, 2012.

53. Izambert, O., Mitton, D., Thourot, M., and Lavaste, F. Dynamic stiffness and damping of human intervertebral disc using axial oscillatory displacement under a free mass system. Eur Spine J **12,** 562, 2003.

54. Smeathers, J.E., and Joanes, D.N. Dynamic compressive properties of human lumbar intervertebral joints: a comparison between fresh and thawed specimens. J Biomech **21,** 425, 1988.

55. Kaigle, A., Ekström, L., Holm, S., Rostedt, M., and Hansson, T. *In vivo* dynamic stiffness of the porcine lumbar spine exposed to cyclic loading: influence of load and degeneration. J Spinal Disord **11,** 65, 1988.

56. Iatridis, J.C., Furukawa, M., Stokes, I.A., Gardner-Morse, M.G., and Laible, J.P. Spatially resolved streaming potentials of human intervertebral disk motion segments under dynamic axial compression. J Biomech Eng **131,** 031006, 2009.

57. Meakin, J.R., and Hukins, D.W. Effect of removing the nucleus pulposus on the deformation of the annulus fibrosus during compression of the intervertebral disc. J Biomech **33,** 575, 2000.

58. Gadd, M.J., and Shepherd, D.E.T. Viscoelastic properties of the intervertebral disc and the effect of nucleus pulposus removal. J Eng Med **225,** 335, 2011.

59. Meakin, J.R., Reid, J.E., and Hukins, D.W. Replacing the nucleus pulposus of the intervertebral disc. Clin Biomech (Bristol, Avon) **16,** 560, 2001.

60. Boxberger, J.I., Orlansky, A.S., Sen, S., and Elliott, D.M. Reduced nucleus pulposus glycosaminoglycan content alters intervertebral disc dynamic viscoelastic mechanics. J Biomech **42,** 1941, 2009.

Address correspondence to:
Barbara Pui Chan, PhD
Tissue Engineering Laboratory
Department of Mechanical Engineering
The University of Hong Kong
Room 711, Haking Wong Building
Pokfulam Rd.
Hong Kong 852
China

E-mail: bpchan@hku.hk

This article has been cited by:

1. Young Sook Lee, Kwang Suk Lim, Jung-Eun Oh, A-Rum Yoon, Wan Seok Joo, Hyun Soo Kim, Chae-Ok Yun, Sung Wan Kim. 2015. Development of porous PLGA/PEI1.8k biodegradable microspheres for the delivery of mesenchymal stem cells (MSCs). *Journal of Controlled Release* **205**, 128-133. [CrossRef]

2. Daisuke Sakai, Gunnar B. J. Andersson. 2015. Stem cell therapy for intervertebral disc regeneration: obstacles and solutions. *Nature Reviews Rheumatology* . [CrossRef]

3. Daisuke Sakai, Sibylle Grad. 2014. Advancing the cellular and molecular therapy for intervertebral disc disease. *Advanced Drug Delivery Reviews* . [CrossRef]